Journal of Medicinal Chemistry

pubs.acs.org/jmc

Drug Annotation

Discovery and Optimization of the First Highly Effective and Orally Available Galectin-3 Inhibitors for Treatment of Fibrotic Disease

Fredrik R. Zetterberg,* Alison MacKinnon,* Thomas Brimert, Lise Gravelle, Richard E. Johnsson, Barbro Kahl-Knutson, Hakon Leffler, Ulf J. Nilsson, Anders Pedersen, Kristoffer Peterson, James A. Roper, Hans Schambye, Robert J. Slack, and Susan Tantawi

Cite This: *J. Med. Chem.* 2022, 65, 12626–12638

Read Online

ACCESS | Metrics & More | Article Recommendations | Supporting Information

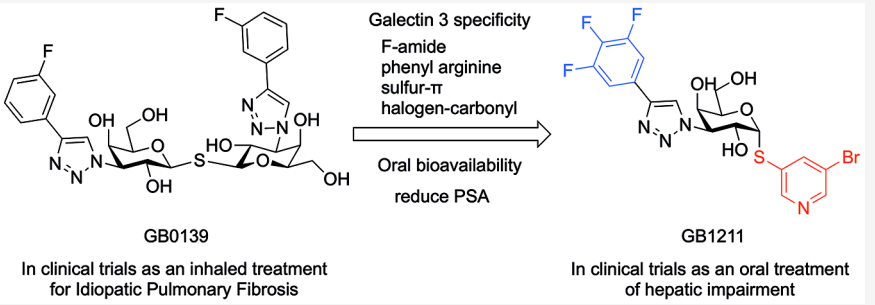

ABSTRACT: Galectin-3 is a carbohydrate-binding protein central to regulating mechanisms of diseases such as fibrosis, cancer, metabolic, inflammatory, and heart disease. We recently found a high affinity (nM) thiodigalactoside GB0139 which currently is in clinical development (PhIIb) as an inhaled treatment of idiopathic pulmonary fibrosis. To enable treatment of systemically galectin-3 driven disease, we here present the first series of selective galectin-3 inhibitors combining high affinity (nM) with oral bioavailability. This was achieved by optimizing galectin-3 specificity and physical chemical parameters for a series of disubstituted monogalactosides. Further characterization showed that this class of compounds reduced profibrotic gene expression in liver myofibroblasts and displayed antifibrotic activity in CCl_4-induced liver fibrosis and bleomycin-induced lung fibrosis mouse models. On the basis of the overall pharmacokinetic, pharmacodynamic, and safety profile, GB1211 was selected as the clinical candidate and is currently in phase IIa clinical trials as a potential therapy for liver cirrhosis and cancer.

INTRODUCTION

Galectins are a class of carbohydrate-binding proteins defined by the specificity of the carbohydrate-recognition (CRD) with conserved sequence motifs and affinity to β-D-galactopyranosides.[1] There are 15 known galectins in mammals, divided into three classes: (1) prototype existing as monomers or dimers of the CRD; (2) chimera consisting of a single CRD and proline/glycine-rich tail; (3) tandem repeat consisting of two distinct CRDs. Galectin-3 is the only member of the chimera class of galectins and is involved in many biological processes such as cell proliferation, angiogenesis, cell adhesion, apoptosis, and mRNA processing and is key to disease processes associated with, for example, cancer and fibrosis.[2]

Galectin-3 is a key regulator of chronic inflammation in the lung, liver, and kidney and in the tumor microenvironment where it also instigates macrophage type change, angiogenesis, T-cell anergy, and immune escape.[3] Galectin-3-deficent mice are protected from fibrosis which results in reduced scarring after injury.[4−6] In tissue fibrosis the major source of collagen is myofibroblast differentiation. This process is is regulated by galectin-3, in addition, galectin-3 is also involved in macrophage polarization.[7,8] Galectin-3 secreted from macrophages activates myofiborblasts and amplifies the pro-fibrotic loop.[7] Furthermore, galectin-3 has been demonstrated to be significantly elevated in fibrotic tissue in patients with chronic liver disease.[9] Most cancers overexpress galectin-3, and high galectin-3 levels in the tumor or in serum signals worse prognosis and worse response to checkpoint inhibitors.[10]

There have been many efforts to develop galectin-3-binding inhibitors, including large biomolecules such as monoclonal antibodies, natural galactose-based polymers such as pectins, synthetic multivalent ligands, and small ligands. Most of these have either or both low affinity and/or limited oral bioavailability.[1,11] The majority of work toward developing small molecules has been based on mono- or disugar themes

Received: April 26, 2022
Published: September 26, 2022

https://doi.org/10.1021/acs.jmedchem.2c00660
J. Med. Chem. 2022, 65, 12626−12638

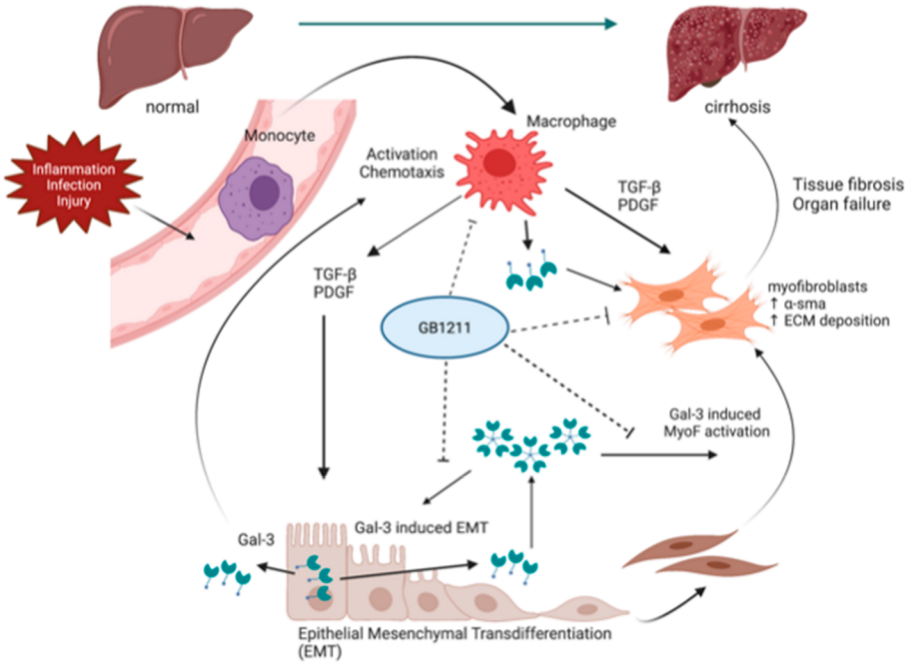

Figure 1. GB1211 inhibits macrophage- and myofibroblast-driven fibrosis in cirrothic liver disease. Monocytes differentitiate into macrophages upon activation via, for example, inflammation, infection, or injury. This results in the release of TGFβ, PDGF, and galectin-3 which results in differentiation of epithelial cells into myofibroblasts which in turn release αSMA and deposit ECM. Galectin-3 is the key mediator in driving the continued macrophage/myofibroblast-driven fibrosis which in a disease state may result in fibrotic liver disease such as cirrhosis.[27]

Scheme 1. Synthesis of Thiodigalactosides 3, 4, and 5a,b[a]

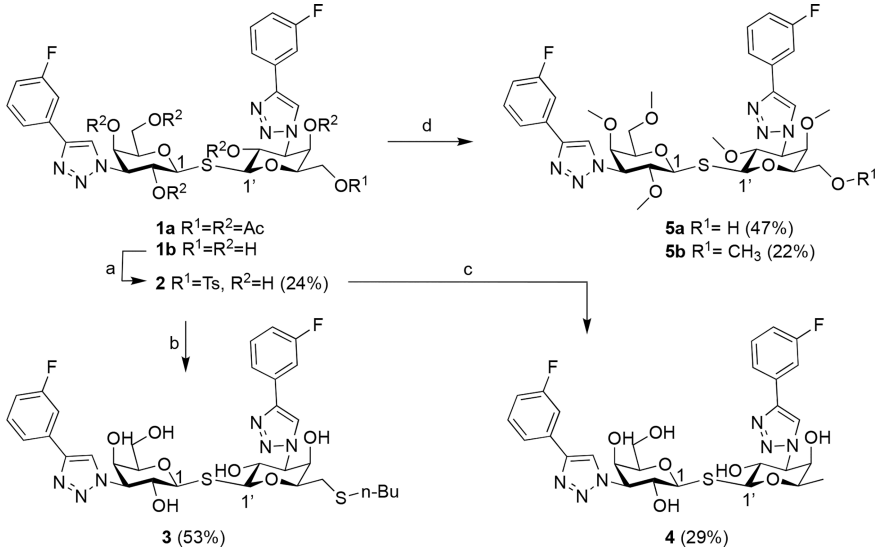

[a]Reagents and conditions: (a) TsCl, pyridine, 37°C, overnight; (b) n-Bu-SH, Cs_2CO_3, DMF, rt, 1 h; (c) $LiAlH_4$, THF, rt, 6 h; (d) (i) NaOMe, MeOH, rt, 2.5 h; (ii) MeI, NaH, DMF, rt, overnight.

with a β-D-galactopyranoside as the common denominator. Most of these efforts have resulted in inhibitors with affinities in, at best, micromolar range. There are exceptions, and the first specific examples of small galectin-3 inhibitors with low-nanomolar affinities are the thiodigalactosides.[12,13] One compound from this class, GB0139 **1b** (previously TD139), is currently in phase 2b clinical trials (ClinicTrials.gov Identifier: NCT03832946) as an inhaled treatment for idiopathic pulmonary fibrosis (IPF). GB0139 has limited oral bioavailability due to high polarity, and in our efforts to develop an oral galectin-3 inhibitor we recently discovered a new class of 1,3-substituted α-D-monogalactopyranosides with surprisingly high affinity for galectin-3.[14] A compound (GB1107) was recently shown to inhibit the growth of lung adenocarcinoma after oral administration.[15] In addition, following our own efforts, several patent applications have recently been published which cover new classes of small high-affinity monogalactopyranosides.[16−28]

In the present study we report the discovery of a new class of orally available small molecule galectin-3 inhibitors and the optimization program leading to the selection of GB1211 as a clinical candidate; this compound has recently completed a

https://doi.org/10.1021/acs.jmedchem.2c00660
J. Med. Chem. 2022, 65, 12626−12638

first-in-human phase 1 clinical trial in healthy subjects and commenced phase 2 clinical development in patients with hepatic impairment (ClinicTrials.gov Identifier: NCT05009680). We will herein describe the optimization of affinity and pharmacokinetic (PK) properties of these novel oral galectin-3 inhibitors, demonstrate inhibiton of the galectin-3-driven macrophage/myofibroblast axis in liver fibrosis, and demonstrate their impact on CCl_4-induced liver fibrosis in mice. The identification of these new galectin-3 inhibitors opens the possibility to test the clinical potential of galectin-3 inhibition systemically, for example targeting fibrotic disorders such as liver (liver cirrhosis), renal and cardiac fibrosis, and cancers. (Figure 1)

RESULTS AND DISCUSSION

Thiodigalactosides such as GB0139 (**1b**, Scheme 1) have low-nanomolar affinities toward galectin-3 and were therefore evaluated as a starting point in the search for orally available inhibitors.[12]

Oral Bioavilability of GB0139 (1b) Is Limited Both by Uptake in the Intestine and by Elimination. The oral bioavailability of **1b** in rat and mice is <1%, and in addition the systemic clearance (CL) after intravenous (iv) administration (2 mg/kg) in mice is 22 mL/min/kg corresponding to 15−18% of the mouse liver blood flow which could be improved upon. In a biodistribution study in mice, ^{14}C-labeled **1b** is excreted via feces, suggesting that **1b** is cleared via a biliary pathway.[28] Further, **1b** (Table 1) has low permeability in both directions across CACO-2 cells, which could be explained by high polarity as expressed in polar surface area (PSA).[29]

Table 1. Galectin-3 Affinity, Permeability, Polar Surface Area, and Lipophilicity Determined for Thiodigalactosides 1b−5b[a]

compound	galectin-3 K_d (μM)[a]	CACO-2 (A > B/B > A) Papp (10^{-6} cm/s)[b]	PSA[c] (Å^2)	log D (pH 7.4)[d]
1b[30]	0.0023[30]	0.07/0.05	201	2.1
3	0.056 ± 0.008	0.06/1.7	181	3.4
4	0.003 ± 0.0009	0.07/0.11	181	2.4
5a	>100	<0.7/56	146	-
5b	>100	27/72	135	-

[a]K_d was determined by fluorescence polarization.[14,32] [b]Permeability (Papp) was determined as permeability over CACO-2 cells from the apical (A) to basolateral side (B) and vice versa.[35] [c]Polar surface area was calculated according to Ertl[29] within the database solution LiveDesign, Schrodinger. [d]Log D was determined by measuring the distribution of compound between 10 mM potassium phosphate buffer (pH 7.4) and octanol using a standard shakeflask method.

Reducing Ligand Polarity Results in Increased Permeability over CACO-2 Membranes. It is well established that the passive permeability over cell membranes is low for highly polar compounds.[33,34] In addition, they also tend to be substrates for transporters, potentially resulting in high renal or biliary clearance and generally low bioavailability after oral administration. The main contributors to the polarity of thiodigalactosides are the hydroxyl groups; thus, substitution or removal of any hydroxy group not involved in the interaction with galectin-3 may result in high affinity combined with improved oral bioavailability.[36] According to the published X-ray structure of galectin-3 (C-terminal domain) complexed with **1b** (GB0139, PDB 5E89, Figure 2), C4, C6, and C2′ hydroxy of **1b** participate in direct interaction with the CRD. Thus, it was hypothesized that the remaining hydroxy groups at positions C2, C4′, and C6′ could either be masked by substitution or removed without substantial loss of galectin-3 affinity. To investigate this, compounds **3**−**5b** were made (Scheme 1).

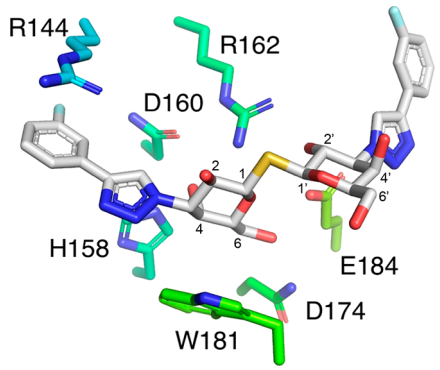

Figure 2. GB0139 (**1b**) complexed with galectin-3 (PDB 5E89). Selected key interacting galectin-3 side chains are shown as sticks, and galactoside carbon numbering used herein is defined. C1−C6 (denoted 1−6 in the figure) of the symmetrical GB0139 are the carbons of the galactopyranose-positioned stacking onto W181, while C1′−C6′ (denoted 1′−6′ in the figure) are the galactopyranose carbons positioned close to E184.

Thiodigalactosides **3**, **4**, and **5a** were made according to Scheme 1. Monotosylation of the C-6 position of **1b**[12] followed by nucleophilic substitution of **2** with n-Bu-SH resulted in **3**. Reduction of **2** using $LiAlH_4$ gave **4**. Deprotection of **1a**[12] using sodium methoxide directly followed by alkylation using MeI gave a mixture of **5a** and **5b**, each of which could be isolated using HPLC.

Introduction of a substituent in the C-6′ position, **3**, resulted in a 24-fold reduction of affinity compared to **1b** whereas removal of the C-6′ hydroxy, **4**, resulted in similar affinity. This confirms that one of the C-6 hydroxy group of one of the galactosides is not necessary for obtaining high affinity. As expected, methylated compounds **5a** and **5b** have no affinity toward galectin-3 because the crucial interactions between the galactoside hydroxyls in positions C4, C6, and C2′ and the CRD of galectin-3 are blocked by methyl groups. Despite reducing the PSA and/or increasing the lipophilicity, neither compound **3** nor **4** shows improved permeability in the CACO-2 assay over **1b**. Compounds **3** and **5a** showed efflux, indicating active transport. Only fully methylated compound **5b** had high permeability over CACO-2 cells in both directions. This made us conclude that it is very difficult to develop an orally available thiodigalactoside with high affinity toward galectin-3.

By determining the permeability of representatives of our in-house library of galectin inhibitors over CACO-2 cells, we found that compounds with a PSA < 140 Å^2 (Figure 3) had medium to high permeability, while compounds with a PSA > 140 Å^2 had low permeability which aligns well with established data for small molecules.[29,33,34] The highest permeability was observed for monogalactosides and in particular for a series of 1,3-disubstituted β-D-monogalactopyranosides; therefore, this series was investigated further using a randomly selected library of aromatic thiols represented by substituted aromatic mono- and bicycles in an attempt to improve affinity (Table 2 and

https://doi.org/10.1021/acs.jmedchem.2c00660
J. Med. Chem. 2022, 65, 12626−12638

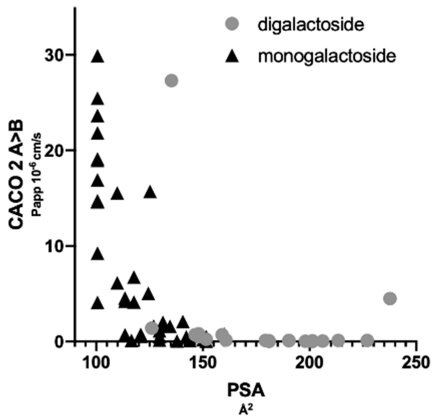

Figure 3. Relationship between polar surface area (PSA Å^2) and permeability (Papp over CACO-2 cells from apical to basolateral A > B 10^{-6} cm/s) for monogalactoside and digalactoside galectin-3 inhibitors.

Scheme 2). In general these compounds had a flat SAR with affinities in the 3−20 μM range.

Table 2. Galectin-3 Affinity, Permeability, and Polar Surface Determined for 3-Substituted 1-Thio-β-D-galactopyranosides 8a−c[a]

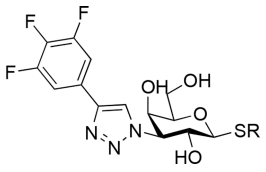

compound	R	galectin-3 K_d (μM)[a]	CACO-2 (A > B/B > A) Papp (10^{-6} cm/s)[b]	PSA (Å^2)[c]
8a	4-acetamidophenyl	3.2 ± 0.26	<0.14/3.9	130
8b	3-methoxyphenyl	1.7 ± 0.36	6.2/24	110
8c[31]	4-methylphenyl	5.2[31]	30/29	101

[a]K_d was determined by fluorescence polarization.[14,32] [b]Permeability (Papp) was determined as permeability over CACO-2 cells from the apical (A) to basolateral side (B) and vice versa.[35] [c]Polar surface area was calculated according to Ertl[29] within the database solution LiveDesign, Schrodinger.

Compounds **8a** and **b** were synthesized starting from 1,2,4,6-tetra-*O*-acetyl-3-azido-3-deoxy-β-D-galactopyranoside **6**[37] using the respective arylthiol mediated by BF_3−OEt_2, resulting in **7a,b**. These were reacted further with trimethyl-[2-(3,4,5-trifluorophenyl)ethynyl]silane, followed by methanolysis of the acetates to give compounds **8a** and **8b** (Scheme 2).

Compounds **8a−c** (Table 2) are in the low-micromolar range of galectin-3 affinity, which is the highest affinity we have observed for 3-substituted aryl 1-thio-β-D-monogalactopyranoside monosaccharides. The permeability and efflux over CACO-2 membranes correlates with the calculated PSA for compounds **8a−c**. The most polar of the compounds, **8a**, has a PSA = 130 Å^2, which results in low permeability and efflux over CACO-2 membranes. By reducing the polarity of the aglycon to less polar groups such as compounds **8b** and **8c**, the permeability is improved and efflux reduced. In effect, **8c** demonstrates similar permeability over CACO-2 membranes in both directions.

Achieving High Galectin-3 Affinity Combined with Oral Bioavailability. Although the β-D-monogalactopyranosides **8b** and **8c** have high permeability over CACO-2 cells, the affinities toward galectin-3 were at best in the single-digit micromolar range. This led us to investigate the bioavailability for an analogue series of 1,3-substituted α-D-monogalactopyranosides. Remarkably, high affinity and specificity were observed for this series of compounds, which may be explained by specific interactions such as fluorine−amide, phenyl−arginine, sulfur−π, and halogen−carbonyl which has been previously discussed.[14] This collection of interactions allows for ligand nanomolar affinities in the difficult to target shallow and amphiphilic binding site of galectin-3 previously only achievable with more polar ligands, for example thiodigalactosides such as **1b**.

Subsequently, additional analogues were synthesized, aiming at optimizing the specific interactions while balancing polarity and lipophilicity (Scheme 2). The α-D-galactopyranosides **11a** and **11d** were made from 2,4,6-tri-*O*-acetyl-3-azido-3-deoxy-β-D-galactopyranosyl chloride **9**[14] by a nucleophilic substitution at the anomeric center with the corresponding aryl thiol to give **10a** and **10d**. These were then reacted in a similar fashion to **7a** and **7b** to give the α-D-galactopyranosides **11a** and **11d**.

X-ray analysis of this new series (not shown) revealed the formation of a halogen bond between a phenyl aglycon *m*-halo substituent and the backbone carbonyl of Gly182 of galectin-3, vitually identical to that observed previously.[14] Halogen bonds can form between an electropositive σ-hole on the halide and the electronegative carbonyl oxygen lone pair. The strength of a halogen bond may be modulated by enhancing the electropositive character of the halide σ-hole, which, for example, can be achieved by introduction of electron-withdrawing groups on the aryl aglycon.[38−40] These kinds of optimizations are difficult to account for because possible electronic and steric constraints also have to be taken into account. Compound **11a** lacks this meta-substituted halogen resulting in about a 10-fold lower affinity for galectin-3 than observed for **11b−d** (Table 3). The highest affinity was observed for **11d** followed by **11c** and **11a**. Although the affinities are similar for **11b−d**, the lipophilicity range spans almost 2 log units (3−4.6), with **11d** combining the highest affinity with the lowest lipophilicity; thus, **11d** has the highest lipophilic efficiency. This suggests that lipophilicity is not the major contributor to affinity for this series of compounds.

The permeability over CACO-2 cells for α-D-galactopyranosides (**11a−d**) correlated with the PSA in a similar fashion to what was observed for β-D-galactopyranosides **8a−c**. Compound **11a** with a PSA of 130 Å^2 had low permeability and efflux. Decreasing the PSA to 124 Å^2 (**11c**) or 114 Å^2 (**11d**) resulted in a medium permeability, whereas **11b** with a PSA of 101 Å^2 resulted in high permeability.

α-D-Monogalactopyranoside Monosaccharides Have High Oral Bioavailability in Mice. To further understand the PK properties, in vitro stability of **11b−d** was evaluated in human and mouse hepatocytes (Table 4). These compounds all displayed low metabolism in human hepatocytes, with the highest stability observed for compound **11d**.

Encouraged by the medium-to-high permeability over CACO-2 cells and good hepatic stability of **11b−d** in both human and mice, the PK properties of these compounds were assessed in mice following a single oral or iv administration. (Table 4) All three compounds displayed high oral bioavailability with **11c** having the highest at 95% and **11d**

https://doi.org/10.1021/acs.jmedchem.2c00660
J. Med. Chem. 2022, 65, 12626−12638

Scheme 2. Synthesis of Compounds 8a, 8b, 11a, and 11d[a]

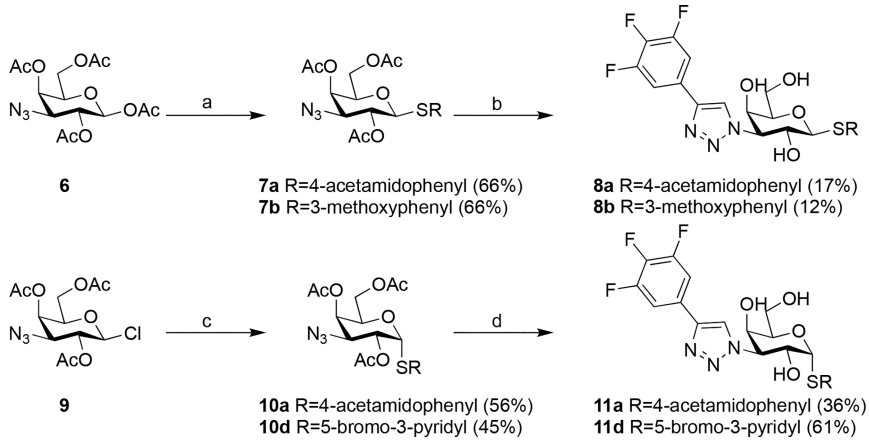

[a]Reagents and conditions: (a) R-SH, $BF_3{\cdot}OEt_2$, mol sieves, DCM, rt; (b) (i) trimethyl-[2-(3,4,5-trifluorophenyl)ethynyl]silane, CuI, Et_3N, DMF, 100 °C; (ii) NaOMe, MeOH, rt; (c) R-SH, NaH, DMF, 50 °C; (d) (i) trimethyl-[2-(3,4,5-trifluorophenyl)ethynyl]silane, CuI, DIPEA or Et_3N, CsF, MeCN or DMF, rt; (ii) NaOMe, MeOH, rt.

Table 3. Galectin-3 Affinity, Permeability, Polar Surface Area, and Lipophilicity Determined for α-D-Monogalactopyranosides 11a–d[a]

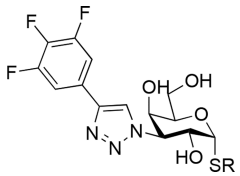

compound	R	galectin-3 (μM)[a]	CACO-2 (A > B/B > A) Papp (10^{-6} cm/s)[b]	PSA (Å^2)[c]	log D (pH 7.4)[d]	LiPE[e]
11a	4-acetamidophenyl	0.38 ± 0.030	0.5/13	130	2.28	4.1
11b	3,4-dichlorophenyl	0.037 ± 0.0010	14/16	101	4.6	2.8
11c	3-chloro-4-cyanophenyl	0.047 ± 0.0063	5/32	124	3.7	3.6
11d	5-bromo-3-pyridyl	0.025 ± 0.0017	4.6/30	114	3.0	4.6

[a]K_d was determined by fluorescence polarization.[14,32] [b]Permeability (Papp) was determined as permeability over CACO-2 cells from the apical (A) to basolateral side (B) and vice versa.[35] [c]Polar surface area was calculated according to Ertl[29] within the database solution LiveDesign, Schrodinger. [d]Log D was determined by measuring the distribution of compound between 10 mM potassium phosphate buffer (pH 7.4) and octanol using a standard shakeflask method. [e]Lipophilic efficiency was calculated as LipE = pK_d − log D (pH 7.4).

Table 4. Mouse Pharmacokinetic Parameters Determined for α-D-Galactopyranosides 11b–d

compound	h-hepatic Clint (μL/min/10^6 cells)[a]	m-hepatic CLint (μL/min/10^6 cells)[a]	in vivo PK mouse CL (mL/min/kg)	F% in vivo PK mouse	Vd L/kg	Fu % protein binding in humans	Fu % protein binding in mice	log D (pH 7.4)
11b	0.7	0.8	1.2	75	0.4	0.2	0.78	4.6
11c	0.8	1.1	3.9	95	0.9	0.8	1.3	3.7
11d	0.15	1.1	10.6	68	1.1	3.9	4.2	3.0

[a]In vitro hepatic CLint was determined by measuring the stability half-life of the respective compounds in human or mouse hepatocytes. The PK experiments were performed by single dose administration orally and iv. The PK parameters were determined by noncompartmental analysis using the PK software PK solutions 2.0, Summit Research Services. CL, clearance; CLint, intrinsic clearance; F%, bioavailability; Fu, fraction unbound; h-hepatic, human hepatic; m-hepatic, mouse hepatic; Vd, volume of distribution.

Table 5. Affinities of Compounds 11b–d toward Galectin-1, -3, -4N, -4C, -8N, -8C, -9N, and -9C

	galectin K_d (μM)[a]							
compound	1	3	4N	4C	8N	8C	9N	9C
11b	3.7 ± 0.33	0.037 ± 0.0010	2.9 ± 0.40	0.13 ± 0.012	83 ± 17	11.0 ± 1.9	2.7 ± 0.24	2.4 ± 0.41
11c	5.18 ± 0.33	0.048 ± 0.0063	3.22 ± 0.40	0.191 ± 0.027	108.7 ± 7.3	22.1 ± 1.5	3.19 ± 0.24	4.28 ± 0.22
11d	3.17 ± 0.16	0.025 ± 0.0017	1.82 ± 0.24	0.092 ± 0.013	125.5 ± 25.5	8.9 ± 0.9	1.61 ± 0.15	1.94 ± 0.16

[a]K_d was determined by fluorescence polarization.[14,32]

the lowest at 68%. The in vivo clearance was lowest for **11b** and somewhat higher for **11c** and **11d**; thus, higher lipophilicity and lower PSA correlate with high systemic exposure after oral administration. Mouse hepatic clearance was found to be very similar between **11b–d** in vitro. In contrast, in vivo mouse clearance differed between the

https://doi.org/10.1021/acs.jmedchem.2c00660
J. Med. Chem. 2022, 65, 12626–12638

compounds, with **11d** having a 10-fold higher clearance than **11b**; this might be explained by the differences in free fraction but might also suggest that alternate clearance mechanisms such as biliary and renal clearance could be involved.

Compounds 11b−d Are Selective Galectin-3 Inhibitors. Compounds **11b−d** were >100-fold selective for other human galectins with the exception of galectin-4C (C terminal domain) where a 2−4-fold selectivity was observed (Table 5).

In addition to affinity being determined by fluorescence polarization (FP), human and mouse galectin-1 and -3 affinity and kinetics were also investigated in a surface plasmon resonance (SPR) assay (Supporting Information, S15). The K_d values correlated very well with to those observed in the FP assay, with fast association and dissociation kinetics (Supporting Information Table S1).

In Vitro Safety Assessment toward a Panel of Targets Indicates a Clean Profile for Compound 11d but Not 11b. The specificity of compound **11b** and **11d** was tested against a panel of 87 different targets (enzymes, receptors, and ion channels, Supporting Information, S20), part of a safety screen provided by Eurofins. No significant hits (>50% inhibition at 10 μM) were found for **11d** whereas **11b** had low affinity toward a few targets (rat calcium L-channel [50−60% dependent on ligand], 82% toward the human dopamine transporter [DAT, 82%] and serotonin [5-hydroxytryptamine] [$5HT_{2B}$] receptors [50%]).

Compound 11d Has Low CYP P450 Inhibition. The inhibition of cytochrome P450s (CYP; 1A2, 2B6, 2C19, 2C9, 2D6, and 3A4) by compounds **11b−d** was also tested. The more lipophilic **11b** and **11c** had >10 μM affinity toward most CYPs apart from **11c** having affinity toward 2B6 (8 μM) and **11b** affinities against 2C8 (6.7 μM), 2C9 (6.52 μM), and 2D6 (8.7 μM). Compound **11d** had no inhibition (>10 μM) toward any CYP.

In Vitro and In Vivo Assessment of Effects on the Human Ether-a-Go-Go-Related Gene (hERG) Suggests Potential hERG Liability for 11b but Not 11d. The binding affinity to the hERG channel was determined to be >10 μM for **11b** or **11d** in pan-screens as referenced above. In a patch clamp assay, **11b** was assessed to have potential hERG liability (S26), which was also confirmed in a guinea pig study where a dose-dependent increase in corrected QT intervals up to 15 ms was observed for **11b** at 3, 10, and 30 μM (Supporting Information, S27).

Compound **11d** had the higher affinity and hepatic stability compared to **11b**. In addition the overall more favorable in vitro safety panel, CYP, and hERG profile of **11d** resulted in selection of **11d** (also named GB1211) as a potential clinical candidate and was characterized further in a range of in vitro and in vivo test systems to measure inhibition of galectin-3.

GB1211, 11d, Inhibits Galectin-3 Production on THP-1 Macrophages and TGFβ-Stimulated Pro-fibrotic Gene Expression In Vitro. Functional inhibition of galectin-3 was investigated in a number of cellular systems. Before testing **11d** in functional assays, cell cytotoxicity was determined in an MTT (3-[4,5-dimethylthiazol-2-yl]-2,5 diphenyltetrazolium bromide) assay. No cell cytotoxicity was observed for **11d** at the concentrations subsequently tested in the functional cellular systems (Supporting Information Table S2). Human monocyte THP1 cells were differentiated into macrophages and incubated with a range of **11d** concentrations for 2 h (h) prior to measurement of cell surface galectin-3 by flow cytometry.[8] **11d** inhibited galectin-3 expression with a potency (IC_{50}) of 220.3 ± 92.0 nM (Figure 4).

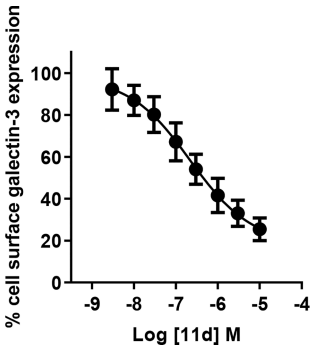

Figure 4. Inhibition of galectin-3 expression on THP1 macrophages by compound **11d**. Percentage cell surface galectin-3 surface expression measured by flow cytometry. Data represent the mean ± standard error of the mean (SEM) of four independent experiments.

Compound **11d** was assessed for its ability to inhibit fibrosis-related gene expression in a human liver stellate cell line (LX2) in vitro. Cells were incubated for 24 h with TGFβ and a range of concentrations of **11d**, and gene expression assessed by quantitative polymerase chain reaction (qPCR). **11d** inhibited TGFβ-induced expression of *Col1A2*, *α-SMA*, *TIMP1*, and *LGalS3* (Figure 5).

The Mouse Galectin-3 Affinity of Galactosides Substituted with a Phenyltriazole at C3 Is in General Lower Compared to Human Galectin-3 (Table 6). This is most likely due to the difference in human and mouse protein sequence 144−150, in particular position 146, which is an alanine in human galectin-3 and a sterically more demanding valine (V160) in mouse galectin-3.[41] A recent publication showcasing X-ray structures on a related series further supports this hypothesis.[42,43]

Structural Analysis of 11d Complexed with Human and Mouse Galectin-3. Compound **11d** was cocrystallized with human galectin-3 C-terminal domain essentially as described previously,[14] and the X-ray structure of **11d** complexed with human galectin-3 C-terminal domain was solved at 1.05 Å (PDB 7ZQX). The X-ray structure revealed a virtually identical ligand pose and interaction pattern to that of the published structure of the **11b** complex (Figure 6A). In addition, **11d** was computationally modeled in complex with mouse galectin-3 to investigate if mouse V160 interfered with efficient **11d** interactions. Briefly, **11d** was placed in the mouse galectin-3 binding site with its galactopyranose ring overlapping the position of the 3-fluorphenyltriazolyl-galactopyranose of GB0139 stacking onto W195 in the GB0139-mouse galectin-3C X-ray complex (PDB 7CXB[42]) and with the bromopyridyl aglycon in a conformation placing the *m*-bromo substituent in a position interacting with mG196 analogous to that of the *m*-chloro substituent of **11b** interacting with G182 in the published human galectin-3 X-ray structure (PDB 6EOL).[14] Energy minimization with MacroModel (OPLS4) implemented in Maestro (v2021−3, Schödinger Inc.) revealed a complex in which the **11d** bromo−mG196 interaction, W195 stacking, and hydrogen bond pattern were retained, but the larger sized mV160 induced a tilt of the **11d** trifluorophenyl moiety, in turn preventing its stacking with mR158 (Figure 6B). Hence, the proposed detrimental effect of mV160 in mouse galectin-3 on phenyltriazolyl-galactoside arginine

https://doi.org/10.1021/acs.jmedchem.2c00660
J. Med. Chem. 2022, 65, 12626−12638

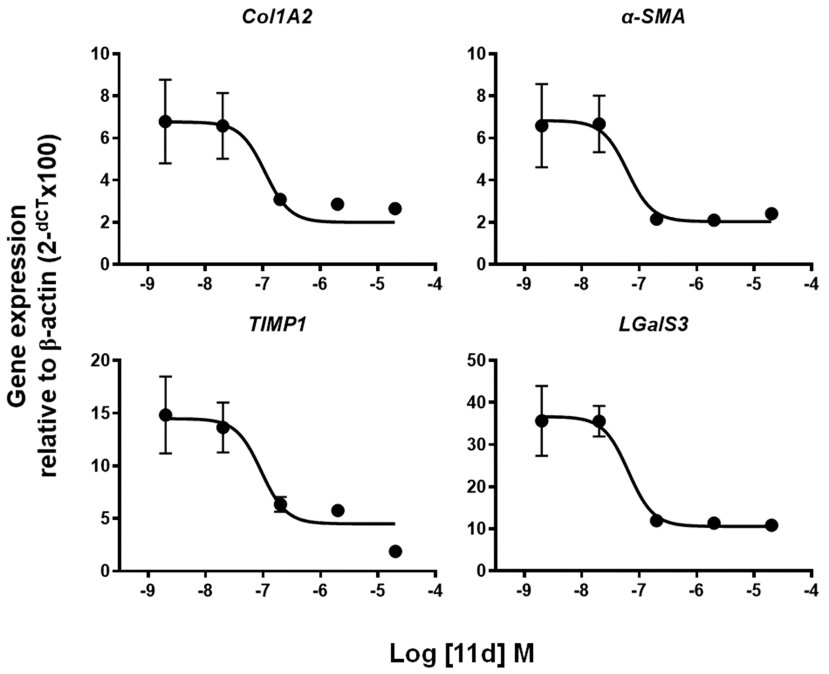

Figure 5. Inhibition of TGFβ stimulated pro-fibrotic gene expression by compound **11d**. Human liver fibroblasts (LX2 cells) were incubated with 2 ng/mL TGFβ and a range of concentrations of **11d** for 24 h prior to RNA extraction and transcript analysis by qPCR. Results are expressed as the relative expression of *Col1A2*, *α-SMA*, *TIMP1*, and *LgalS3* relative to *β-actin*. Data represent the mean ± SEM of four independent experiments.

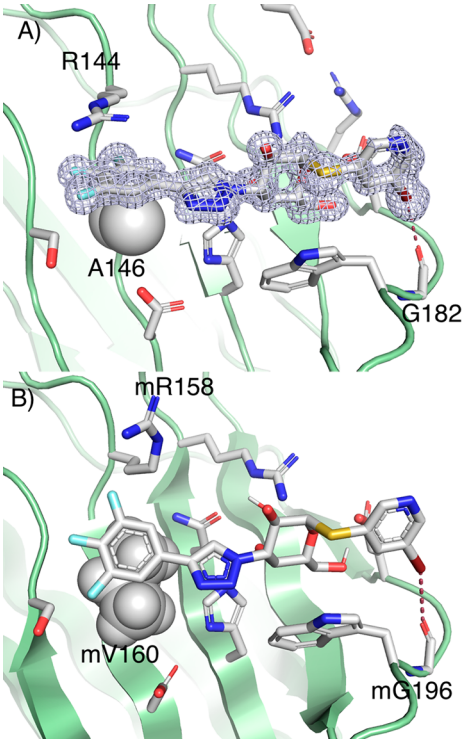

Figure 6. Panel A: GB1211 (**11d**) complexed with human galectin-3C (PDB 7ZQX). Panel B: GB1211 (**11d**) docked in a published structure of mouse galectin-3C (PDB 7CXB).[42]

stacking interactions and affinities[5,6,43] most likely plays a role for **11d** as well (Figure 6B).

Compound 11d Reduces Fibrosis In Vivo Using Murine Models. Given the lower affinity of **11d** for mouse galectin-3 (Table 6), doses of up to 10 mg/kg twice daily (bid) for **11d** were selected to ensure that plasma levels were above

Table 6. Human and Mouse Galectin-3 Affinities of 11b and 11d

	galectin-3 K_d (μM)	
compound	human	mouse
11b	0.037 ± 0.0010	1.8 ± 0.07
11d	0.025 ± 0.0017	0.77 ± 0.06

mouse galectin-3 K_d in order to investigate whether blocking galectin-3 function might improve liver fibrosis in vivo mouse models. Hence, **11d** was orally administered (2 mg/kg or 10 mg/kg bid based on its in vivo PK profile) (Supporting Information Figure S1) to mice during the last 4 weeks of an 8-week regimen of twice-weekly CCl_4 injections (1 μL/g of a 1:3 CCl_4:olive oil mix intraperitoneally [ip]). Compound **11d** significantly reduced fibrotic collagen deposition in the hepatic parenchyma as assessed by picrosirius red (PSR) staining at 10 mg/kg (Figure 7). In addition, compound **11d** significantly reduced collagen deposition in the lungs of bleomycin-treated mice following dosing bid from days 12 to 26 post bleomycin instillation (Supporting Information Figure S2).

CONCLUSIONS

Thiodigalactosides such as GB0139 (**1b**) have high galectin-3 specificity but low oral bioavailability due to high polarity. Attempts to improve the oral bioavailability by reducing polarity through simple substitution or removal of hydroxylic groups gave little or no improvement in permeability over CACO-2 cell membranes. By screening a selection of our in-house library of representative mono- and digalactoside galectin-3 inhibitors over CACO-2 cells, the permeability A > B was shown to correlate to the polarity as determined by PSA. A recent series of β-D-galactopyranoside monosaccharides was identified to have good permeability, but attempts to optimize the affinity for this series resulted in compounds with, at best, micromolar affinity. Meanwhile, a new series of α-D-

https://doi.org/10.1021/acs.jmedchem.2c00660
J. Med. Chem. 2022, 65, 12626−12638

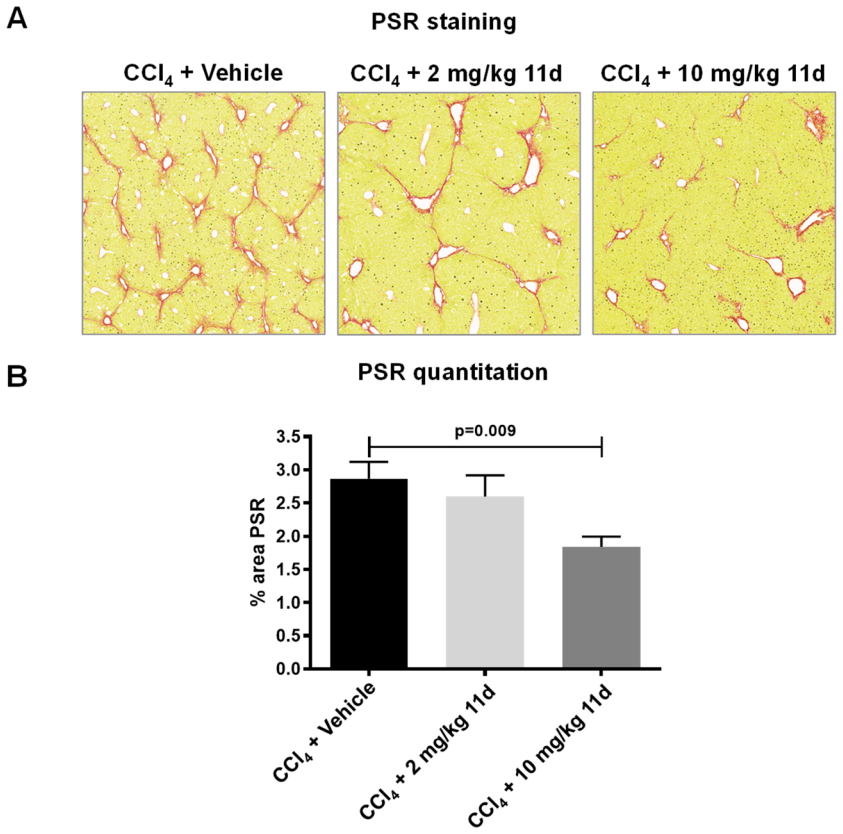

Figure 7. Effect of compound **11d** dosing on liver PSR staining in a mouse CCl_4-induced liver fibrosis model. Mice received 1 μL/g of 25% CCl_4 diluted in olive oil ip twice-weekly for 8 weeks with compound **11d** dosed orally bid during the last 4 weeks (n = 8 per group). Representative PSR-stained sections of mouse liver (A) and quantitation of PSR-stained sections (B) are shown. Data were analyzed by one-way ANOVA.

galactopyranoside monosaccharides was discovered to combine high permeability over CACO-2 cells with two-digit nanomolar affinity toward galectin-3. Optimizing the lipophilic efficiency for this series of compounds resulted in **11d**, a highly selective, orally available galectin-3 inhibitor with no in vitro safety signals in the Eurofins safety screen, CYP P450s, hERG, or micronucleus studies. Compound **11d** inhibited galectin-3 expression on human macrophages and inhibited profibrotic gene expression induced by TGFβ in human stellate cells with a potency that paralelled its affinity in binding assays. Compound **11d** was shown to be orally bioavailable in mice and reduced CCl_4-induced liver fibrosis and bleomycin-induced lung fibrosis when administered in a therapeutic dosing regimen. On the basis of the overall profile, compound **11d** (also known as GB1211) was selected as a clinical candidate. GB1211 was found to be well tolerated in healthy subjects[44] and is currently in clinical development as a novel, orally active therapy for liver fibrosis (NCT03809052) and cancer (NCT05240131).

EXPERIMENTAL SECTION

Chemistry. *General Procedures.* Nuclear magnetic resonance (NMR) spectra were recorded on a Bruker Avance II 400 MHz, 400 MHz Varian, 500 MHz Bruker AVANCE III 500, or 500 MHz Bruker Avance Neo 500 instrument, at ambient temperature. Chemical shifts are reported in ppm (δ) using the residual solvent as internal standard. Peak multiplicities are expressed as follow: s, singlet; d, doublet; dd, doublet of doublets; t, triplet; dt, doublet of triplet; q, quartet; m, multiplet; br s, broad singlet. HRMS were determined by direct infusion on a Waters XEVO-G2 QTOF mass spectrometer using electrospray ionization (ESI). LC-MS were acquired on an Agilent 1100 or Agilent 1200 HPLC coupled with an Agilent MSD mass spectrometer operating in ES(+) ionization mode. Columns: Waters symmetry 2.1 × 30 mm C18, Chromolith RP-18 2 × 50 mm or XBridge C18 (4.6 × 50 mm, 3.5 μm), or SunFire C18 (4.6 × 50 mm, 3.5 μm). Solvent A water + 0.1% TFA and solvent B MeCN + 0.1% TFA. Wavelength: 254 nm. Preparative HPLC was performed on a Gilson system. (A) Flow: 10 mL/min column: kromasil 100-5-C18 column. Wavelength: 254 nm. Solvent A water + 0.1% TFA and solvent B MeCN + 0.1% TFA. (B) On a Gilson 215. Flow: 25 mL/min column: XBrige prep C18 10 μm OBD (19 × 250 mm) column. Wavelength: 254 nm. Solvent A water (10 mM ammonium hydrogen carbonate) and solvent B MeCN. Flash chromatography was performed on a Biotage SP1 automated system, using Biotage Snap KP-Sil 25 or 50 g cartridges. Compounds **3**−**5b**, **8a**−**c**, and **11a**−**d** were of >95% purity according to HPLC (Agilent series 1100 system, column Eclipse XDB-C18, 0.8 mL/min H_2O−MeCN gradient 5−95% 13 min with 0.1% TFA).

*3,3′-Dideoxy-3,3′-bis[4-(3-fluorophenyl)-1H-1,2,3-triazol-1-yl]-6-(4-methylphenyl)sulfonyl-1,1′-sulfanediyl-di-β-D-galactopyranoside (**2**).* Compound **1b** (673 mg, 1.04 mmol) was dissolved in pyridine (20 mL). *p*-Toluenesulfonyl chloride (550 mg, 2.88 mmol) was added and the mixture stirred overnight at 37 °C. The mixture was concentrated in vacuo. Water (5 mL) was added and the mixture concentrated in vacuo. The residue was purified on silica, eluting with EtOAc/MeOH 1:0 → 1:4 to afford compound **2** (223 mg, 24%). ^{1}H NMR ($(CD_3)_2SO$, 500 MHz) δ 8.54 (s, 1H), 8.52 (s, 1H), 7.75 (d, J = 8.3 Hz, 2H), 7.62 (d, J = 7.8 Hz, 2H), 7.57 (dt, J = 10.1, 2.2 Hz, 2H), 7.42 (tt, J = 8.0, 5.7 Hz, 2H), 7.31 (d, J = 8.1 Hz, 2H), 7.06 (dtd, J = 10.9, 8.4, 2.0 Hz, 2H), 4.94−4.87 (m, 4H), 4.77 (q, J = 10.5 Hz, 2H), 4.25−4.20 (m, 2H), 4.20−4.14 (m, 3H), 3.84 (q, J = 8.3, 7.3 Hz, 2H), 3.72 (td, J = 9.0, 7.1 Hz, 1H), 2.36 (s, 3H). ^{13}C NMR ($(CD_3)_2SO$, 125 MHz) δ 164.3, 164.2, 162.3, 145.9, 145.8, 145.7, 145.4, 133.0, 132.9, 132.8, 132.4, 130.6, 130.5, 129.8, 127.6, 121.0, 114.5, 114.3, 111.8, 111.7, 85.1, 84.9, 80.0, 76.6, 69.1, 68.3, 68.0, 67.4,

https://doi.org/10.1021/acs.jmedchem.2c00660
J. Med. Chem. 2022, 65, 12626−12638

67.0, 66.7, 61.4, 20.2. HRMS calculated for $[C_{35}H_{37}F_2N_6O_{10}S_2]^+$: 803.1981; found: 803.1982.

*6-S-Butyl-3,3′,6-trideoxy-3,3′-bis[4-(3-fluorophenyl)-1H-1,2,3-triazol-1-yl]-1,1′-sulfanediyl-di-β-D-galactopyranoside (**3**).* Cesium carbonate (190 mg, 0.58 mmol) was weighed into a flask under nitrogen. Compound **2** (60 mg, 0,075 mmol) was dissolved in DMF (10 mL) in a second flask, and 1-butanethiol (100 μL, 0.93 mmol) was added to this solution. The resulting solution was added to the flask with cesium carbonate. The resulting mixture was stirred 1 h at rt. The mixture was diluted with brine (100 mL) and extracted with diethyl ether (100 mL). The organic phase was washed with brine (3 × 100 mL), dried, and concentrated in vacuo. The residue was purified by column chromatography (SiO_2/EtOAc). One fraction was isolated and concentrated in vacuo. The residue was dissolved in 1,4-dioxane and lyophilized to give compound **3** (29 mg, 53%). ^{1}H NMR (CD_3OD, 500 MHz) δ 8.57 (s, 1H, Ph), 8.56 (s, 1H, Ph), 7.67−7.62 (m, 2H, Ph), 7.59 (ddd, *J* = 10.1, 2.4, 1.6 Hz, 2H, Ph), 7.43 (tdd, *J* = 7.9, 6.0, 1.9 Hz, 2H, Ph), 7.09−7.03 (m, 2H, Ph), 4.97−4.88 (m, 4H, H-1, H-1′, H-3 and H-3′), 4.75−4.67 (m, 2H, H-2 and H-2′), 4.26 (d, *J* = 2.6 Hz, 1H, H-4 or H-4′), 4.18 (d, *J* = 2.7 Hz, 1H, H-4 or H-4′), 3.97 (t, *J* = 7.1 Hz, 1H, H-5), 3.92−3.82 (m, 2H, H-5′ and H-6′), 3.73 (dd, *J* = 11.3, 4.5 Hz, 1H, H-6′), 2.89 (dd, *J* = 13.5, 6.6 Hz, 1H, H-6), 2.79 (dd, *J* = 13.5, 7.2 Hz, 1H, H-6), 2.65−2.60 (m, 2H, CH_2), 1.62−1.53 (m, 2H, CH_2), 1.44−1.38 (m, 2H, CH_2), 0.91 (t, *J* = 7.4 Hz, 3H, CH_3). ^{13}C NMR (CD_3OD, 125 MHz) δ 164.3, 162.3, 145.8, 133.0, 132.9, 130.5, 121.1, 121.0, 114.5, 114.3, 111.9, 111.7, 85.0, 84.8, 80.0, 78.8, 68.7, 68.4, 67.6, 67.5, 67.0, 66.9, 61.4, 32.0, 31.9, 31.6, 21.5, 12.6. HRMS calculated for $[C_{32}H_{39}F_2N_6O_7S_2]^+$: 721.2290; found: 721.2288.

*3,3′,6-Trideoxy-3,3′-bis[4-(3-fluorophenyl)-1H-1,2,3-triazol-1-yl]-1,1′-sulfanediyl-di-β-D-galactopyranoside (**4**).* To a solution of compound **2** (108 mg, 0.14 mmol) in THF (10 mL) under nitrogen was added lithium aluminum hydride (29 mg, 0.75 mmol), and the mixture was stirred 6 h at rt. The reaction was quenched with water (30 μL). NaOH (15% aq, 90 μL) and water (90 μL) were added, and the mixture was filtered and concentrated. The residue was purified by preparative HPLC to afford compound **4** (25 mg, 29%). ^{1}H NMR (CD_3OD, 500 MHz) δ 8.56 (s, 2H, Ph), 7.67−7.62 (m, 2H, Ph), 7.59 (dt, *J* = 10.0, 1.9 Hz, 2H, Ph), 7.47−7.40 (m, 2H, Ph), 7.06 (td, *J* = 8.6, 2.6 Hz, 2H, Ph), 4.93−4.87 (m, 4H, H-1, H-1′, H-3 and H-3′), 4.71 (t, *J* = 10.1 Hz, 1H, H-2 or H-2′), 4.66 (t, *J* = 10.1 Hz, 1H, H-2 or H-2′), 4.16 (d, *J* = 2.7 Hz, 1H, H-4 or H-4′), 4.01 (q, *J* = 6.2 Hz, 1H, H-5), 3.94 (d, *J* = 2.6 Hz, 1H, H-4 or H-4′), 3.90−3.81 (m, 2H, H-5′ and H-6′), 3.72 (dd, *J* = 11.3, 4.3 Hz, 1H, H-6′), 1.34 (d, *J* = 6.4 Hz, 3H, H-6). ^{13}C NMR (CD_3OD, 125 MHz) δ 164.3, 162.3, 145.8, 132.9, 130.5, 130.4, 121.1, 121.0, 121.0, 114.4, 114.3, 111.8, 111.6, 85.2, 84.9, 80.1, 75.5, 70.8, 68.4, 67.7, 67.4, 67.0, 66.8, 61.4, 15.7. HRMS calculated for $[C_{28}H_{31}F_2N_6O_7S]^+$: 633.1943; found: 633.1946.

*3,3′-Dideoxy-3,3′-bis[4-(3-fluorophenyl)-1H-1,2,3-triazol-1-yl]-2,2′,4,4′,6-penta-O-methyl-1,1′-sulfanediyl-di-β-D-galactopyranoside (**5a**) and 3,3′-Dideoxy-3,3′-bis[4-(3-fluorophenyl)-1H-1,2,3-triazol-1-yl]-2,2′,4,4′,6,6′-hexa-O-methyl-1,1′-sulfanediyl-di-β-D-galactopyranoside (**5b**).* Compound **1a** (502 mg, 0.56 mmol) was suspended in MeOH (10 mL), and sodium methoxide (23 mg, 0.43 mmol) was added. After 1.5 h, more sodium methoxide (10 mg, 0.19 mmol) was added, and after 1 h, the mixture was filtered. To the filtrate was added water (100 mL), and the resulting precipitate was collected by filtration, washed with water, and dried in vacuo to afford a white solid (95 mg). Some of the obtained material (45 mg, 0.063 mmol) was dissolved in DMF (5 mL). Sodium hydride (60% in mineral oil, 13 mg, 0.31 mmol) was added followed by iodomethane (20 μL, 0.32 mmol). The mixture was stirred at rt overnight, diluted with water (5 mL), filtered, and purified by preparative HPLC to afford compound **5a** (21 mg, 47%) and compound **5b** (9.9 mg, 22%).

*Analytical Data for Compound **5a**.* ^{1}H NMR ($(CD_3)_2SO$, 500 MHz) δ 8.99 (s, 2H, Ph), 7.78 (d, *J* = 7.8 Hz, 2H, Ph), 7.75−7.71 (m, 2H, Ph), 7.55−7.50 (m, 2H, Ph), 7.19 (td, *J* = 8.9, 2.5 Hz, 2H, Ph), 5.19 (dd, *J* = 10.6, 3.0 Hz, 2H, H-3 and H-3′), 5.08 (d, *J* = 9.7 Hz, 1H, H-1 or H-1′), 4.97 (d, *J* = 9.7 Hz, 1H, H-1 or H-1′), 4.93 (dd, *J* = 6.6, 4.6 Hz, 1H, OH-6′), 4.07−4.00 (m, 3H, H-2, H-2′ and H-5), 3.83 (t, *J* = 6.8 Hz, 1H, H-5′), 3.72 (d, *J* = 3.3 Hz, 1H, H-4 or H-4′), 3.67 (d, *J* = 3.1 Hz, 1H, H-4 or H-4′), 3.65−3.60 (m, 1H, H-6′), 3.56−3.48 (m, 3H, H-6 and H-6′), 3.33 (s, 3H, CH_3), 3.24 (s, 3H, CH_3), 3.24 (s, 3H, CH_3), 2.97 (s, 3H, CH_3), 2.95 (s, 3H, CH_3). ^{13}C NMR ($(CD_3)_2SO$, 125 MHz) δ 164.1, 162.1, 145.8, 133.7, 133.6, 131.6, 131.5, 122.2, 121.6, 115.1, 115.0, 112.3, 112.1, 81.9, 79.1, 79.0, 78.7, 77.0, 76.8, 76.5, 70.4, 65.0, 64.9, 61.0, 59.8, 58.9. HRMS calculated for $[C_{33}H_{41}F_2N_6O_8S]^+$: 719.2675; found: 719.2677.

*Analytical Data for Compound **5b**.* ^{1}H NMR ($(CD_3)_2SO$, 500 MHz) δ 8.99 (s, 2H, Ph), 7.78 (d, *J* = 7.8 Hz, 2H, Ph), 7.75−7.71 (m, 2H, Ph), 7.52 (td, *J* = 8.0, 6.4 Hz, 2H, Ph), 7.18 (td, *J* = 8.5, 2.2 Hz, 2H, Ph), 5.21 (dd, *J* = 10.6, 3.2 Hz, 2H, H-3 and H-3′), 4.99 (d, *J* = 9.7 Hz, 2H, H-1 and H-1′), 4.08−4.00 (m, 4H, H-2, H-2′, H-5 and H-5′), 3.68 (d, *J* = 3.1 Hz, 2H, H-4 and H-4′), 3.52 (qd, *J* = 9.8, 6.6 Hz, 4H, H-6 and H-6′), 3.33 (s, 6H, CH_3), 3.24 (s, 6H, CH_3), 2.95 (s, 6H, CH_3). ^{13}C NMR ($(CD_3)_2SO$, 125 MHz) δ 164.1, 162.1, 145.8, 133.7, 133.6, 131.6, 131.5, 122.2, 121.6, 115.1, 115.0, 112.3, 112.1, 82.2, 79.1, 76.9, 76.5, 70.5, 64.8, 61.0, 59.8, 58.9. HRMS calculated for $[C_{34}H_{43}F_2N_6O_8S]^+$: 733.2831; found: 733.2831.

*4-Acetamidophenyl 2,4,6-Tri-O-acetyl-3-azido-3-deoxy-1-thio-β-D-galactopyranoside (**7a**).* To a solution of 1,2,4,6-tetra-*O*-acetyl-3-azido-3-deoxy-β-D-galactopyranoside (200 mg, 0.54 mmol) in DCM (15 mL) were added *N*-(4-mercaptophenyl)acetamide (270 mg, 1.61 mmol) and molecular sieves (4 Å). The mixture was stirred 15 min at rt followed by cooling to 0 °C. Boron trifluoride etherate (0.68 mL, 5.36 mmol) was added, and the mixture was stirred 6 h at rt. The reaction was quenched with saturated aqueous $NaHCO_3$, and the phases were separated. The organic layer was purified by column chromatography on silica (DCM:MeOH 100:1, 50:1) to afford compound **7a** (170 mg, 66%). ^{1}H NMR ($CDCl_3$, 400 MHz): 7.49−7.47 (m, 4H, Ph), 5.43 (d, *J* = 2.0 Hz, 1H, H-4), 5.17 (t, *J* = 8.0 Hz, 1H, H-2), 4.61 (d, *J* = 8.0 Hz, 1H, H-1), 4.14−4.10 (m, 2H, H-6), 3.87−3.84 (m, 1H, H-5), 3.62 (dd, *J* = 8.0, 2.4 Hz, H-3), 2.19 (s, 3H, CH_3), 2.18 (s, 3H, CH_3), 2.14 (s, 3H, CH_3), 2.01 (s, 3H, CH_3). MS calculated for $[C_{20}H_{25}N_4O_8S]^+$: 481.1; found: 481.1

*4-Acetamidophenyl 3-Deoxy-3-[4-(3,4,5-trifluorophenyl)-1H-1,2,3-triazol-1-yl]-1-thio-β-D-galactopyranoside (**8a**).* To a solution of compound **7a** (170 mg, 0.35 mmol) in dry DMF (10 mL) were added triethylamine (0.25 mL, 1.77 mmol), copper iodide (20 mg, 0,11 mmol), and trimethyl-[2-(3,4,5-trifluorophenyl)ethynyl]silane (162 mg, 0,71 mmol), and the mixture was stirred 30 min at 100 °C. Water was added, the mixture was filtered, and the filtrate was extracted with ethyl acetate. The organic phase was washed with water and brine, dried, and concentrated. The residue was purified by column chromatography, and the obtained product was dissolved in MeOH (5 mL). A sodium methoxide solution (30%, 7.9 mg, 0.044 mmol) was added, and the mixture was stirred 1 h at rt. Dowex 50WX8 ion-exchange resin was added (pH = 9), and the mixture was filtered. The filtrate was purified by preparative HPLC to give compound **8a** (30 mg, 17%). ^{1}H NMR (CD_3OD, 400 MHz): δ 8.49 (s, 1H, Ph), 7.64 (dd, *J* = 9.0, 6.6 Hz, 2H, Ph), 7.56 (m, 4H, Ph), 4.87 (dd, *J* = 10.4, 3.1 Hz, 1H, H-3), 4.76 (d, *J* = 9.5 Hz, 1H, H-1), 4.25 (dd, *J* = 10.5, 9.5 Hz, 1H, H-2), 4.12 (d, *J* = 2.9 Hz, 1H, H-4), 3.84−3.70 (m, 3H, H-5 and H-6), 2.13 (s, 3H, CH_3). ^{13}C NMR (CD_3OD, 100 MHz): δ 171.7, 139.7, 134.1, 129.6, 122.8, 121.4, 110.8, 91.6, 80.9, 69.6, 69.3, 67.9, 62.3, 23.8. HRMS calculated for $[C_{22}H_{22}F_3N_4O_5S]^+$, 511.1263; found: 511.1263.

*3-Methoxyphenyl 3-Deoxy-3-[4-(3,4,5-trifluorophenyl)-1H-1,2,3-triazol-1-yl]-1-thio-β-D-galactopyranoside (**8b**).* Compound **8b** was made from compound **6** (240 mg) using a procedure similar to that for **8a**, resulting in an overall yield of 30 mg, 12%. ^{1}H NMR (CD_3OD, 500 MHz): 8.50 (s, 1H, Ph), 7.64 (dd, *J* = 8.8, 6.6 Hz, 2H, Ph), 7.25−7.20 (m, 2H, Ph), 7.15−7.12 (m, 1H, Ph), 6.86−6.82 (m, 1H, Ph), 4.91−4.86 (m, 2H, H-1 and H-3), 4.33−4.28 (m, 1H, H-2), 4.14 (d, *J* = 2.8 Hz, 1H, H-4), 3.87 (t, *J* = 6.0 Hz, 1H, H-5), 3.83−3.78 (m, 4H, H-6 and CH_3), 3.74 (dd, *J* = 11.3, 5.5 Hz, 1H, H-6). ^{13}C NMR (CD_3OD, 125 MHz): 161.4, 136.8, 130.7, 124.2, 122.8, 117.0, 114.5, 110.9, 110.7, 91.2, 81.0, 69.6, 69.3, 67.8, 62.4, 55.8. MS calculated for $[C_{21}H_{21}F_3N_3O_5S]^+$: 484.1; found: 484.0.

https://doi.org/10.1021/acs.jmedchem.2c00660
J. Med. Chem. 2022, 65, 12626−12638

*5-Bromopyridin-3-yl 2,4,6-Tri-O-acetyl-3-azido-3-deoxy-1-thio-α-D-galactopyranoside (**10d**).* NaH (82.99 mg, 3.47 mmol) was added to a solution of 5-bromopyridine-3-thiol (658.67 mg, 3.47 mmol) in DMF (10 mL) at 0 °C. The solution was stirred at rt for 30 min. Then compound **9** (1.01 g, 2.89 mmol) was added. The mixture was stirred at 50 °C for 2 h followed by cooling to rt. Water (50 mL) was added, and the mixture was extracted with EtOAc (15 mL × 3). The combined organic layers were washed with brine, dried over Na_2SO_4, and concentrated in vacuo to afford crude product, which was purified by biotage (EtOAc/PE = 5−40%, ISCO 40 g, 30 mL/min, silica gel, UV 254 nm) to afford compound **10d** (650 mg, 45%). ^{1}H NMR ($CDCl_3$, 400 MHz): δ 8.51 (d, J = 2.0 Hz, 1H, Ph), 8.49 (d, J = 2.0 Hz, 1H, Ph), 7.90 (t, J = 2.0 Hz, 1H, Ph), 5.90 (d, J = 5.6 Hz, 1H, H-1), 5.42 (d, J = 2.8 Hz, 1H, H-4), 5.22 (dd, J = 10.8, 5.4 Hz, 1H, H-2), 4.56 (dd, J = 7.6, 4.8 Hz, 1H, H-5), 4.09−4.03 (m, 1H, H-6), 3.98−3.86 (m, 2H, H-3 and H-6), 2.13 (s, 3H, CH_3), 2.10 (s, 3H, CH_3), 1.97 (s, 3H, CH_3). MS calculated for $[C_{17}H_{20}BrN_4O_7S]^+$: 503.0; found: 503.0.

*5-Bromopyridin-3-yl 3-Deoxy-3-[4-(3,4,5-trifluorophenyl)-1H-1,2,3-triazol-1-yl]-1-thio-α-D-galactopyranoside (**11d**).* To a solution of compound **10d** (650 mg, 1.29 mmol) in DMF (15 mL) were added trimethyl-[2-(3,4,5-trifluorophenyl)ethynyl]silane (442.22 mg, 1.94 mmol), copper iodide (73.78 mg, 0.39 mmol), CsF (294.26 mg, 1.94 mmol), and triethylamine (653.39 mg, 6.46 mmol). The reaction vessel was purged three times with nitrogen. The reaction mixture was stirred at rt for 2 h. The mixture was filtered and washed with EtOAc (50 mL). The filtrate was concentrated in vacuo. The obtained material was dissolved in MeOH (10.0 mL) followed by addition of NaOMe (7.46 mg, 0.14 mmol). The mixture was stirred at rt for 1 h followed by acidification to pH 5−6 using Dowex 50W X8 hydrogen form. The reaction mixture was filtered, washed with MeOH (20 mL), and concentrated in vacuo to afford crude product, which was purified by preparative HPLC to afford compound **11d** (445 mg, 61%). ^{1}H NMR (CD_3OD, 400 MHz): δ 8.69 (d, J = 1.9 Hz, 1H, Ph), 8.58 (d, J = 2.1 Hz, 1H, Ph), 8.56 (s, 1H, Ph), 8.36 (t, J = 2.0 Hz, 1H, Ph), 7.66 (dd, J = 8.9, 6.6 Hz, 2H, Ph), 5.93 (d, J = 5.2 Hz, 1H, H-1), 5.02 (dd, J = 11.4, 2.8 Hz, 1H, H-3), 4.94 (dd, J = 11.4, 5.2 Hz, 1H, H-2), 4.48 (dt, J = 6.1, 1.0 Hz, 1H, H-5), 4.20 (dd, J = 2.8, 1.0 Hz, 1H, H-4), 3.73 (dd, J = 11.5, 5.4 Hz, 1H, H-6), 3.69 (dd, J = 11.5, 6.7 Hz, 1H, H-6). ^{13}C NMR (CD_3OD, 100 MHz): δ 151.2, 149.6, 144.2, 135.2, 122.9, 121.9, 110.8, 90.9, 73.8, 69.6, 66.6, 65.4, 62.0. HRMS calculated for $[C_{19}H_{17}BrF_3N_4O_4S]^+$, 533.0106; found: 533.0107.

*4-Acetamidophenyl 3-deoxy-3-[4-(3,4,5-trifluorophenyl)-1H-1,2,3-triazol-1-yl]-1-thio-α-D-galactopyranoside (**11a**).* Compound **10a** was made from compound **9** (283 mg) using a procedure similar to that for **10d**, resulting in a yield of 219 mg, 56%. To a solution of compound **10a** (216 mg, 0.45 mmol) in MeCN (15 mL) were added copper iodide (52 mg, 0.27 mmol) and trimethyl-[2-(3,4,5-trifluorophenyl)ethynyl]silane (0.121 mL, 0.90 mmol) followed by DIPEA (0.079 mL, 0.45 mmol). The mixture was stirred 6 h at rt. Brine was added and the mixture was extracted three times with diethyl ether. The combined organic phases were washed with brine, dried over Na_2SO_4, and concentrated. The obtained material was dissolved in MeOH (50 mL) followed by addition of NaOMe (2.5 mL, 1 M). The mixture was stirred 2 h at rt, acetic acid (2 mL) was added, and the mixture was concentrated. The residue was purified by preparative HPLC to afford compound **11a** (85 mg, 36%). ^{1}H NMR (CD_3OD, 400 MHz): δ 8.54 (s, 1H, Ph), 7.66 (dd, J = 9.0, 6.6 Hz, 2H, Ph), 7.56 (m, 4H, Ph), 5.69 (d, J = 5.3 Hz, 1H, H-1), 4.98 (dd, J = 11.4, 2.8 Hz, 1H, H-3), 4.88 (obscured by water, 1H, H-2), 4.58 (t, J = 6.2 Hz, 1H, H-5), 4.20 (d, J = 2.6 Hz, 1H, H-4), 3.74 (dd, J = 11.5, 5.8 Hz, 1H, H-6), 3.68 (dd, J = 11.5, 5.8 Hz, 1H, H-6), 2.12 (s, 3H, CH_3). ^{13}C NMR (CD_3OD, 100 MHz): δ 171.7, 139.9, 135.1, 129.4, 123.0, 121.5, 110.8, 92.1, 73.0, 69.7, 66.9, 65.6, 62.1, 23.8. HRMS calculated for $[C_{22}H_{22}F_3N_4O_4S]^+$, 511.1263; found: 511.1259.

ADME and Pharmacokinetics. *Human and Mice Hepatic Stability.* Stock solutions of the test compound (10 mM) were prepared in dimethyl sulfoxide (DMSO). Aliquots of stock solutions were diluted to 200 μM with DMSO and then further diluted to 2 μM with KHB buffer. Hepatocytes from various species were seeded at a density of 2 × 10^6 cells/mL and treated with 50 μL of prewarmed 2 μM test compound. At the 0 min time point, 200 μL of ACN containing an internal standard (IS) was added followed by 50 μL of hepatocytes solution before sealing the wells. For all other time points, 50 μL of hepatocytes solution was added to the wells before incubation at 37 °C. At 15, 30, 60, and 120 min, 200 μL of ACN containing IS was added to the wells, respectively, and sealed. After quenching, cells were sonicated for 5 min and then centrifuged at 5594*g* for 15 min (Thermo Multifuge × 3R); 30 μL of supernatant from each well was transferred to a 96-well sample plate containing 150 μL of ultrapure water for LC-MS/MS analysis. The peak area response ratio (PARR) to IS of the compounds at 15, 30, 60, and 120 min was compared to the PARR at 0 min to determine the percent of test compound remaining at each time point. Half-lives were calculated using Excel software, fitting to a single-phase exponential decay equation.

CACO-2 Permeability. CACO-2 cells were seeded on polycarbonate filter inserts (Millipore, CAT#PSHT 010 R5) and grown for 21−28 days prior to the transport experiments. Transepithelial electric resistance (TEER) and Lucifer Yellow permeability were checked before and after the assay. Test compounds were dissolved at 10 mM in DMSO and diluted to 10 μM in Hanks Balanced Salt Solution (HBSS, Invitrogen, cat. no. 14025-092) with 25 mM HEPES, pH 7.4, for each assay; test compounds at 10 μM were used in both the apical-to-basolateral (A-B) and basolateral-to-apical (B-A) directions. Incubations were conducted at 37 °C for 90 min. At the end of incubation, donor samples were diluted by assay buffer and analyzed by LC-MS/MS. The concentrations of the compounds were quantified using a standard curve.

Human and Mouse Plasma Protein Binding. Test compounds were prepared in plasma at 1 μM. Samples were loaded on the donor side, and blank buffer samples were loaded on the receiver side of the equilibrium dialysis device. Samples were incubated in an air-bath shaker at 60 rpm for 5 h at 37 °C and then analyzed by LC-MS/MS.

Lipophilicity Log D (pH 7.4). Test compounds were dissolved in DMSO to a concentration of 10 mM, 10 μL aliquots of each solution were transferred into 2 mL tubes, and 300 μL of octanol was added before sealing the tubes and agitating for 5 min. All samples were then centrifuged at 2000 rpm for 5 min before adding 600 μL of 10 mM potassium phosphate buffer (pH 7.4). All samples were then mixed vigorously for 1 h at rt and then centrifuged at 2000 rpm for 5 min. The octanol and water phases were separated and diluted 2400-fold and 60-fold, respectively. All samples were analyzed by LC-MS/MS.

In Vivo Pharmacokinetics. Mean weight of female C57BL/6 mice (Harlan Europe) included in the experiment was determined to be 19.5 g. Test compounds were administered orally (1 mg/mL) or iv (0.2 mg/mL) via the tail vein in a formulation of 0.5% HPMC in sodium phosphate buffer/citric acid buffer at pH 6.5 or 50% TEG formulation, respectively. Test compounds were administered at hour 0, at a dose of 10 mg/kg orally and l mg/kg iv. Loaded syringes were weighed before and after administration to determine the actual volume given.

Blood was collected from two animals per treatment group and time point and from two naive animals by cardiac puncture, using a syringe and needle, following sacrifice. Collection time points were 15 min, 30 min, 1 h, 2 h, 4 h, 8 h, and 24 h post oral administration and 2 min, 10 min, 30 min, 1 h, 2 h, 4 h, and 8 h post intravenous administration. The blood was collected into ethylenediaminetetraacetic acid (EDTA)-containing microtubes (Microvette 500 K2E tubes) and left at 4 °C for less than 60 min; plasma was separated by centrifugation (830*g*/3000 rpm for 20 min). Plasma was transferred to new 1.5 mL Eppendorf tubes, 120 μL in one tube and remaining plasma in a second tube, and stored at −80 °C until analyzed by HPLC at Red Glead Discovery (Lund, Sweden). HPLC results were analyzed by noncompartmental analyses using the PK Solutions 2.0, Summit Research Services. Concentrations below the lower limit of quantification (LLOQ) were set to half the value of LLOQ (0.5 nmol/L). Values above the upper limit were set as the upper limit in calculations. Average concentrations from each time-point were used for calculations.

https://doi.org/10.1021/acs.jmedchem.2c00660
J. Med. Chem. 2022, 65, 12626−12638

Biology. *Cell Culture.* Human colorectal adenocarcinoma (CACO-2), human THP1 cell line, and human stellate LX2 cell line were obtained from the American Tissue Culture Collection (ATCC, Rockville, MD). Tissue culture reagents were purchased from Invitrogen. Dog and human hepatocytes were purchased from Bioreclamation IVT; mouse, rat, and monkey cells were purchased from Xenotech. CACO-2 cells were maintained in Modified Eagle's Medium (MEM), containing 10% heat-inactivated fetal bovine serum (FBS), and 1% nonessential amino acids. THP1 cells were maintained in RPMI medium containing 10% FBS, 5 μg/mL glutamine, 50 U/mL penicillin, and 50 μg/mL streptomycin, and LX2 cells were cultured in RPMI medium containing 1% FBS, 5 μg/mL glutamine, and 50 U/mL penicillin. All cell lines were grown at 37 °C in a humidified atmosphere at 5% CO_2.

Animals. All animal handling and experiments were performed in accordance with the local Animal Welfare and Ethical Review Body (AWERB) and issued in accordance with the Animals (Scientific Procedures) Act 1986. Male (8−9 weeks) C57BL/6 mice (Harlan Laboratories) were used in the study and were sacrificed by carbon dioxide inhalation before samples were taken at the end of each experiment.

CCl_4-Induced Liver Fibrosis. C57/Bl6J male mice were given twice-weekly intraperitoneal injections of 1 μL/g of 25% CCl_4 (diluted with olive oil) for 8 weeks. The galectin-3 inhibitor **11d** was prepared at a concentration of 1 mg/mL 10% solutol:90% PEG300. Drug was administered orally at a dose of 10 mL/kg twice daily (**11d**) for the last 4 weeks of the CCl_4 treatment period. Livers were removed and processed 24 h after the last dose of CCl_4 and 2 h after the last dose of galectin-3 inhibitor. Liver samples were fixed in 4% neutral-buffered formalin for histological examination.

Immunohistochemistry. Formalin-fixed, paraffin-embedded 4 μM sections were stained with picrosirius red (PSR). Images of PSR staining were acquired using an Axioscan slide scanner. Histological quantifications were performed on 10 regions of the liver (200× total magnification), selected at random using ImageJ software. The number of red pixels was recorded and expressed as a fraction of the total number of pixels, averaged across 10 different regions per section.

Macrophage Galectin-3 Expression. Human THP1 cells were differentiated with 100 ng/mL phorbol 12-myristate 13-acetate (PMA, Sigma-Aldrich) for 24 h, washed, and incubated for 2 h in serum-free media with **11d**. Cells were blocked for 10 min using Human TruStain FcX Receptor Blocking Solution (Biolegend), and cell surface galectin-3 was assessed by incubation with FITC-labeled antigalectin-3 antibody (Cedaralane 1:50 dilution) for 30 min at 4 °C. Cells were washed in 1X phosphate-buffered saline (PBS) and analyzed by flow cytometry using an LSRFortessa flow cytometer (Beckton Dickenson). Data were analyzed using FlowJo software version 10.8.0 (Treestar).

Stellate Cell Activation. LX2 cells were washed and transferred to serum-free medium 2 h prior to treatment for 24 h with **11d** ± 2 ng/mL TGFβ.

Quantitative Real-Time Reverse Transcriptase (RT)-PCR Analysis. RNA was prepared using RNeasy (Qiagen), as per the manufacturer's protocol, and 500 ng of RNA was used for cDNA synthesis using Quantitect Reverse Transcription kit (Qiagen). Quantitative real-time PCR was performed using SYBR Green master mix (Qiagen) and KiCqStart primers (Sigma-Aldrich).

■ ASSOCIATED CONTENT

Supporting Information

The Supporting Information is available free of charge at https://pubs.acs.org/doi/10.1021/acs.jmedchem.2c00660.

NMR spectra and purity chromatograms of synthesized compounds. Additional methods describing surface plasmon resonance (SPR) analysis and cell cytotoxicity. PK profile of **11d** (Figure S1) and the effect of compound **11d** dosing on lung collegen in a murine bleomycin-induced lung fibrosis model (Figure S2). Tables summarizing SPR binding affinity and kinetics for **11d** against human and mouse galectin-1 and -3 (Table S1) and cell cytotoxicity of **11d** in A549 cells (Table S2). Specificity screen of **11d** toward 87 different targets. In vivo assessment of QTc effect of **11b** and **11d** in anesthetized guinea pig. Cocrystallization of galectin-3 C-terminal domain with compound **11d**. Plots of CACO-2 A > B vs PSA and ClogD(7.4) (PDF)

SMILES strings for compounds (CSV)

■ AUTHOR INFORMATION

Corresponding Authors

Fredrik R. Zetterberg − *Galecto Biotech AB, SE-413 46 Gothenburg, Sweden;* orcid.org/0000-0002-7789-8782; Phone: +46 763240495; Email: FZ@galecto.com

Alison MacKinnon − *Galecto Biotech ApS, Edinburgh EH16 4UX, U.K.*; Phone: +44 7711832576; Email: am@galecto.com

Authors

Thomas Brimert − *Red Glead Discovery AB, SE-223 63 Lund, Sweden; Biochemistry and Structural Biology, Center for Molecular Protein Science, Department of Chemistry, Lund University, SE-221 00 Lund, Sweden*

Lise Gravelle − *Galecto Biotech ApS, DK-2200 Copenhagen, Denmark*

Richard E. Johnsson − *Red Glead Discovery AB, SE-223 63 Lund, Sweden*

Barbro Kahl-Knutson − *Biochemistry and Structural Biology, Center for Molecular Protein Science, Department of Chemistry, Lund University, SE-221 00 Lund, Sweden*

Hakon Leffler − *Department of Laboratory Medicine, Lund University, SE-221 00 Lund, Sweden;* orcid.org/0000-0003-4482-8945

Ulf J. Nilsson − *Galecto Biotech AB, SE-413 46 Gothenburg, Sweden; Centre for Analysis and Synthesis, Department of Chemistry, Lund University, SE-221 00 Lund, Sweden;* orcid.org/0000-0001-5815-9522

Anders Pedersen − *Galecto Biotech ApS, DK-2200 Copenhagen, Denmark*

Kristoffer Peterson − *Galecto Biotech AB, SE-413 46 Gothenburg, Sweden; Centre for Analysis and Synthesis, Department of Chemistry, Lund University, SE-221 00 Lund, Sweden*

James A. Roper − *Galecto Biotech ApS, SG1 2FX Hertfordshire, U.K.;* orcid.org/0000-0002-8910-6033

Hans Schambye − *Galecto Biotech ApS, DK-2200 Copenhagen, Denmark*

Robert J. Slack − *Galecto Biotech ApS, SG1 2FX Hertfordshire, U.K.*

Susan Tantawi − *Galecto Biotech ApS, DK-2200 Copenhagen, Denmark*

Complete contact information is available at: https://pubs.acs.org/10.1021/acs.jmedchem.2c00660

Author Contributions

Project conceptualization and design was led by F.Z. in vitro and in vivo. All pharmacology experiments apart from SPR and cell viability experiments were designed and led by A.M. Authors employed by and consulting with Galecto, Inc., participated in the design, study conduct, analysis, and

https://doi.org/10.1021/acs.jmedchem.2c00660
J. Med. Chem. 2022, 65, 12626−12638

interpretation of data, as well as the writing, review, and approval of the manuscript. Authors employed by Red Glead Discovery contributed to compound design and synthesis. The manuscript was written by F.Z. with contributions from all authors. All authors have given approval to the final version of the manuscript.

Funding

GB1211 is being developed by Galecto Inc. This study was funded by Galecto Biotech AB and Galecto APS. Third-party editorial assistance was funded by Galecto Inc.

Notes

The authors declare the following competing financial interest(s): F.Z. and K.P. are employees of Galecto Biotech AB. A.M., L.G., S.T., A.P., R.J.S., J.R., A.P., and H.S. are employees of Galecto APS. F.Z., K.P., A.B., A.M., L.G., S.T., A.P., R.J.S., J.R., A.P., H.L., U.J.N., and H.S. are either option or option/shareholders of Galecto Inc.

■ ACKNOWLEDGMENTS

The authors gratefully acknowledge Cheng Guangwu and his team at Chempartner for synthetic chemistry work. Editorial assistance was provided by Sinéad Holland, Ph.D., of Ashfield MedComms, an Ashfield Health company.

■ ABBREVIATIONS

CACO-2, human colorectal adenocarcinoma cells; Clint, intrinsic clearance; Col1A2, gene coding for pro-α2(I) chain of type 1 collagen; CRD, carbohydrate recognition domain; DIPEA, diisopropylethylamine; EtOAc, ethyl acetate; FP, fluorescence polarization; LGalS3, galectin-3 coding gene; LX2, liver stellate cell; IPF, idiopathic pulmonary fibrosis; MeCN, acetonitrile; Papp, apparent permeability; PARR, peak area response rate; qPCR, quantitative polymerase chain reaction; α-SMA, alpha smooth muscle actin; SPR, surface plasmon resonance; TEG, tetraethylene glycol; TIMP1, metallopeptidase inhibitor 1; TGFβ, transforming growth factor β

■ REFERENCES

(1) Johannes, L.; Jacob, R.; Leffler, H. Galectins at a glance. *J. Cell Sci.* **2018**, *131*. DOI: 10.1242/jcs.208884

(2) Sciacchitano, S.; Lavra, L.; Morgante, A.; Ulivieri, A.; Magi, F.; De Francesco, G. P.; Bellotti, C.; Salehi, L. B.; Ricci, A. Galectin-3: One Molecule for an Alphabet of Diseases, from A to Z. *Int. J. Mol. Sci.* **2018**, *19* (2), 379

(3) Ruvolo, P. P. Galectin 3 as a guardian of the tumor microenvironment. *Biochim. Biophys. Acta* **2016**, *1863* (3), 427−437.

(4) MacKinnon, A. C.; Liu, X.; Hadoke, P. W.; Miller, M. R.; Newby, D. E.; Sethi, T. Inhibition of galectin-3 reduces atherosclerosis in apolipoprotein E-deficient mice. *Glycobiology* **2013**, *23* (6), 654−663.

(5) Mackinnon, A. C.; Gibbons, M. A.; Farnworth, S. L.; Leffler, H.; Nilsson, U. J.; Delaine, T.; Simpson, A. J.; Forbes, S. J.; Hirani, N.; Gauldie, J.; Sethi, T. Regulation of transforming growth factor-beta1-driven lung fibrosis by galectin-3. *Am. J. Respir Crit Care Med.* **2012**, *185* (5), 537−546.

(6) Henderson, N. C.; Mackinnon, A. C.; Farnworth, S. L.; Poirier, F.; Russo, F. P.; Iredale, J. P.; Haslett, C.; Simpson, K. J.; Sethi, T. Galectin-3 regulates myofibroblast activation and hepatic fibrosis. *Proc. Natl. Acad. Sci. U. S. A.* **2006**, *103* (13), 5060−5065.

(7) Henderson, N. C.; Mackinnon, A. C.; Farnworth, S. L.; Kipari, T.; Haslett, C.; Iredale, J. P.; Liu, F. T.; Hughes, J.; Sethi, T. Galectin-3 expression and secretion links macrophages to the promotion of renal fibrosis. *Am. J. Pathol.* **2008**, *172* (2), 288−298.

(8) MacKinnon, A. C.; Farnworth, S. L.; Hodkinson, P. S.; Henderson, N. C.; Atkinson, K. M.; Leffler, H.; Nilsson, U. J.; Haslett, C.; Forbes, S. J.; Sethi, T. Regulation of alternative macrophage activation by galectin-3. *J. Immunol* **2008**, *180* (4), 2650−2658.

(9) Moon, H. W.; Park, M.; Hur, M.; Kim, H.; Choe, W. H.; Yun, Y. M. Usefulness of Enhanced Liver Fibrosis, Glycosylation Isomer of Mac-2 Binding Protein, Galectin-3, and Soluble Suppression of Tumorigenicity 2 for Assessing Liver Fibrosis in Chronic Liver Diseases. *Ann. Lab Med.* **2018**, *38* (4), 331−337.

(10) Capalbo, C.; Scafetta, G.; Filetti, M.; Marchetti, P.; Bartolazzi, A. Predictive Biomarkers for Checkpoint Inhibitor-Based Immunotherapy: The Galectin-3 Signature in NSCLCs. *Int. J. Mol. Sci.* **2019**, *20* (7), 1607−1615.

(11) Blanchard, H.; Yu, X.; Collins, P. M.; Bum-Erdene, K. Galectin-3 inhibitors: a patent review (2008-present). *Expert Opin Ther Pat* **2014**, *24* (10), 1053−1065.

(12) Delaine, T.; Collins, P.; MacKinnon, A.; Sharma, G.; Stegmayr, J.; Rajput, V. K.; Mandal, S.; Cumpstey, I.; Larumbe, A.; Salameh, B. A.; Kahl-Knutsson, B.; van Hattum, H.; van Scherpenzeel, M.; Pieters, R. J.; Sethi, T.; Schambye, H.; Oredsson, S.; Leffler, H.; Blanchard, H.; Nilsson, U. J. Galectin-3-Binding Glycomimetics that Strongly Reduce Bleomycin-Induced Lung Fibrosis and Modulate Intracellular Glycan Recognition. *ChemBioChem.* **2016**, *17* (18), 1759−1770.

(13) Cumpstey, I.; Salomonsson, E.; Sundin, A.; Leffler, H.; Nilsson, U. J. Double affinity amplification of galectin-ligand interactions through arginine-arene interactions: synthetic, thermodynamic, and computational studies with aromatic diamido thiodigalactosides. *Chemistry* **2008**, *14* (14), 4233−4245.

(14) Zetterberg, F. R.; Peterson, K.; Johnsson, R. E.; Brimert, T.; Hakansson, M.; Logan, D. T.; Leffler, H.; Nilsson, U. J. Monosaccharide Derivatives with Low-Nanomolar Lectin Affinity and High Selectivity Based on Combined Fluorine-Amide, Phenyl-Arginine, Sulfur-pi, and Halogen Bond Interactions. *ChemMedChem.* **2018**, *13* (2), 133−137.

(15) Vuong, L.; Kouverianou, E.; Rooney, C. M.; McHugh, B. J.; Howie, S. E. M.; Gregory, C. D.; Forbes, S. J.; Henderson, N. C.; Zetterberg, F. R.; Nilsson, U. J.; Leffler, H.; Ford, P.; Pedersen, A.; Gravelle, L.; Tantawi, S.; Schambye, H.; Sethi, T.; MacKinnon, A. C. An orally active galectin-3 antagonist inhibits lung adenocarcinoma growth and augments response to PD-L1 blockade. *Cancer Res.* **2019**, *79* (7), 1480−1492.

(16) Magnani, J. L.; Peterson, J. M.; Vohra, Y. U.; Ghosh, I.; Nogueira, J.; Sarkar, A. K.; Majumdar, D. Galectin-3 Inhibiting C-Glycoside Ketones, Ethers, and Alcohols. World Patent WO/2021/133924, 2021.

(17) Magnani, J. L.; Peterson, J. M.; Sarkar, A. K.; Vohra, Y. U.; Ghosh, I.; Noguiera, J. Galectin-3 Inhibiting C-Glycosides. World Patent WO/2021/086816, 2021

(18) Liu, C.; Feng, J.; Devasthale, P.; Murugesan, N.; Ellsworth, B. A.; Regueiro-Ren, A.; Nara, S. J.; Jalagam, P. R.; Panda, M. Small Molecule Inhibitors of Galectin-3. World Patent WO/2020/210308, 2020.

(19) Liu, C.; Yoon, D. S.; Wang, W.; Jianxin, F.; Ellsworth, B. A.; Regueiro-Ren, A.. Small Molecule Inhibitors of Galectin-3. World Patent WO/2020/198266, 2020.

(20) Hartz, R. A.; Xu, L.; Yoon, D. S.; Hartz, R. A.; Xu, L.; Yoon, D. S.; Regueiro-Ren, A.; Jalagam, P. R.; Panda, M.; Nair, S. K.. World Patent WO/2019/241461, 2019 December 19.

(21) Jalagam, P. R.; Nair, S. K.; Panda, M.; Regueiro-Ren, A. inventors. Small Molecule Inhibitors of Galectin-3. World Patent WO/2019/075045, 2019.

(22) Jalagam, P. R.; Nair, S. K.; Panda, M.; Feng, J.; Wang, W.; Liu, C.; Ellsworth, B. A.; Sarabu, R.; Swidorski, J.; Hartz, R. A.; Xu, L.; Yoon, D. S.; Beno, B. R.; Regueiro-Ren, A. Small Molecule Inhibitors of Galectin-3. World Patent WO/2019/067702, 2019.

(23) Bolli, M.; Bur, D.; Gatfielda, J.; Grisostomi, C.; Remen, L.; Zumbrunn, C. (Hetero)Aryl-Methyl-Thio-Beta-D-Galactopyranoside Derivatives. World Patent WO/2021/028336, 2021.

(24) Bolli, M.; Gatfield, J.; Grisostomi, C.; Remen, L.; Sager, C.; Zumbrunn, C. 2-Hydroxycycloalkane-1-Carbamoyl Derivatives. World Patent WO/2021/028570, 2021.
(25) Bolli, M.; Gatfield, J.; Grisostomi, C.; Remen, L.; Sager, C.; Zumbrunn, C. Alpha-D-Galactopyranoside Derivatives. World Patent WO/2021/038068, 2021.
(26) Bolli, M.; Bur, D.; Gatfielda, J.; Grisostomi, C.; Remen, L.; Zumbrunn, C. (2-Acetamidyl)Thio-Beta-D-Galactopyranoside Derivatives. World Patent WO/2021/028323, 2021.
(27) Slack, R. J.; Mills, R.; Mackinnon, A. C. The therapeutic potential of galectin-3 inhibition in fibrotic disease. *Int. J. Biochem. Cell Biol.* **2021**, *130*, 105881.
(28) An exploratory biodistribution study of radioactivity in NMRI mice following a single intratracheal, intravenous, or oral administration dose of 14C-TD139 was performed by Charles River, Canada.
(29) Ertl, P.; Rohde, B.; Selzer, P. Fast calculation of molecular polar surface area as a sum of fragment-based contributions and its application to the prediction of drug transport properties. *J. Med. Chem.* **2000**, *43* (20), 3714−3717.
(30) Peterson, K.; Kumar, R.; Stenstroem, O.; Verma, P.; Verma, P. R.; Hakansson, M.; Kahl-Knutsson, B.; Zetterberg, F.; Leffler, H.; Akke, M.; Logan, D. T.; Nilsson, U. J. Systematic Tuning of Fluorogalectin-3 Interactions Provides Thiodigalactoside Derivatives with Single-Digit nM Affinity and High Selectivity. *J. Med. Chem.* **2018**, *61* (3), 1164−1175.
(31) Cumpstey, I.; Carlsson, S.; Leffler, H.; Nilsson, U. J. Synthesis of a phenyl thio-beta-D-galactopyranoside library from 1,5-difluoro-2,4-dinitrobenzene: discovery of efficient and selective monosaccharide inhibitors of galectin-7. *Org. Biomol Chem.* **2005**, *3* (10), 1922−1932.
(32) Sörme, P.; Kahl-Knutsson, B.; Huflejt, M.; Nilsson, U. J.; Leffler, H. Fluorescence polarization as an analytical tool to evaluate galectin-ligand interactions. *Anal. Biochem.* **2004**, *334* (1), 36−47.
(33) Sugano, K.; Kansy, M.; Artursson, P.; Avdeef, A.; Bendels, S.; Di, L.; Ecker, G. F.; Faller, B.; Fischer, H.; Gerebtzoff, G.; Lennernaes, H.; Senner, F. Coexistence of passive and carrier-mediated processes in drug transport. *Nat. Rev. Drug Discov.* **2010**, *9* (8), 597−614.
(34) Palm, K.; Stenberg, P.; Luthman, K.; Artursson, P. Polar molecular surface properties predict the intestinal absorption of drugs in humans. *Pharm. Res.* **1997**, *14* (5), 568−571.
(35) Artursson, P.; Ungell, A. L.; Lofroth, J. E. Selective paracellular permeability in two models of intestinal absorption: cultured monolayers of human intestinal epithelial cells and rat intestinal segments. *Pharm. Res.* **1993**, *10* (8), 1123−1129.
(36) Cramer, J.; Sager, C. P.; Ernst, B. Hydroxyl Groups in Synthetic and Natural-Product-Derived Therapeutics: A Perspective on a Common Functional Group. *J. Med. Chem.* **2019**, *62* (20), 8915−8930.
(37) Lowary, T. L.; Hindsgaul, O. Recognition of synthetic O-methyl, epimeric, and amino analogues of the acceptor alpha-L-Fuc p-(1−>2)-beta-D-Gal p-OR by the blood-group A and B gene-specified glycosyltransferases. *Carbohydr. Res.* **1994**, *251*, 33−67.
(38) Persch, E.; Dumele, O.; Diederich, F. Molecular recognition in chemical and biological systems. *Angew. Chem., Int. Ed. Engl.* **2015**, *54* (11), 3290−3327.
(39) Riley, K. E.; Murray, J. S.; Fanfrlik, J.; Rezac, J.; Sola, R. J.; Concha, M. C.; Ramos, F. M.; Politzer, P. Halogen bond tunability II: the varying roles of electrostatic and dispersion contributions to attraction in halogen bonds. *J. Mol. Model* **2013**, *19* (11), 4651−4659.
(40) Wilcken, R.; Zimmermann, M. O.; Lange, A.; Joerger, A. C.; Boeckler, F. M. Principles and applications of halogen bonding in medicinal chemistry and chemical biology. *J. Med. Chem.* **2013**, *56* (4), 1363−1388.
(41) Salomonsson, E.; Carlsson, M. C.; Osla, V.; Hendus-Altenburger, R.; Kahl-Knutson, B.; Oberg, C. T.; Sundin, A.; Nilsson, R.; Nordberg-Karlsson, E.; Nilsson, U. J.; Karlsson, A.; Rini, J. M.; Leffler, H. Mutational tuning of galectin-3 specificity and biological function. *J. Biol. Chem.* **2010**, *285* (45), 35079−35091.
(42) Kumar, A.; Paul, M.; Panda, M.; Jayaram, S.; Kalidindi, N.; Sale, H.; Vetrichelvan, M.; Gupta, A.; Mathur, A.; Beno, B.; Regueiro-Ren, A.; Cheng, D.; Ramarao, M.; Ghosh, K. Molecular mechanism of interspecies differences in the binding affinity of TD139 to Galectin-3. *Glycobiology* **2021**, *31* (10), 1390−1400.
(43) Xu, L.; Hartz, R. A.; Beno, B. R.; Ghosh, K.; Shukla, J. K.; Kumar, A.; Patel, D.; Kalidindi, N.; Lemos, N.; Gautam, S. S.; Kumar, A.; Ellsworth, B. A.; Shah, D.; Sale, H.; Cheng, D.; Regueiro-Ren, A. Synthesis, Structure-Activity Relationships, and In Vivo Evaluation of Novel Tetrahydropyran-Based Thiodisaccharide Mimics as Galectin-3 Inhibitors. *J. Med. Chem.* **2021**, *64* (10), 6634−6655.
(44) Slack, R. J.; MacKinnon, A. C.; Aslanis, V.; McClinton, C.; Tantawi, S.; Gravelle, L.; Nilsson, U. J.; Leffler, H.; Brooks, A.; Khindri, S. K.; Marshall, R. P.; Pedersen, A.; Schambye, H.; Zetterberg, F. Safety and pharmacokinetics of GB1211, an oral galectin-3 inhibitor: a single- and multiple-dose first-in-human study in healthy participants. Unpublished.

https://doi.org/10.1021/acs.jmedchem.2c00660
J. Med. Chem. 2022, 65, 12626−12638